

# SOME RESULTS ON CONTROL THEORY FOR PROBLEMS IN FLUID DYNAMICS

by **Susana N. Gomes\***

**ABSTRACT.**—I will introduce some concepts in linear control theory, and how to adapt and use them to control some problems modelled by nonlinear partial differential equations appearing in a canonical fluid dynamics setting, showcasing how some simple results tailored for ODEs or linear PDEs can be explored to solve nonlinear complex problems from applications. This is a brief exposition of some of the results in [4] and [10].

Control theory is a branch of applied mathematics and systems engineering which considers dynamical systems, usually ordinary or partial differential equations (ODE/PDEs), and studies the development — or design — of algorithms whose goal is to drive these systems to a desired state while minimising any costs, delays, overshoots, or errors.

The mathematical theory of (feedback) control is outlined in [16, 23], where control of (linear and nonlinear) ordinary differential equations is considered, and where the authors introduce concepts such as controllability (any state can be reached by any starting point), stabilisability (it is possible to drive the system to have stable dynamics), and sufficient conditions for these to be possible. One can also introduce the Linear Quadratic Regulator (LQR), an example of an optimal control problem, where in addition to controlling the system, one also minimises a cost functional, usually penalising deviations from the desired state and the cost of the control. An optimal control problem is solved using the *Pontryagin maximum principle*, which is similar to the first-order optimality conditions (or Karush-Kuhn-Tucker, KKT, conditions) in traditional optimisation.

More recently, the theory of optimal control has been extended to problems modelled by PDEs [21], where one minimises a cost functional subject to the target solution solving a PDE. In this case, when applying the Pontryagin maximum principle, one needs to compute Fréchet derivatives of a Lagrangian, which involves several tools in functional analysis, and so proving existence of optimal controls is a harder task.

While the theory of feedback and optimal control has received extensive attention for systems governed

by ODEs and (linear) PDEs, it was only recently that mathematicians started to target more complex systems, such as, for example, turbulence in fluid dynamics, and in this case, they often resort to the use of reduced-order models (ROM) which use techniques such as principal component analysis (PCA) to simplify the (infinite dimensional) state space into a finite dimensional and tractable vector or Hilbert space. However, in certain applications, we can obtain simplified models based on physical assumptions of the problem, and use these for control design. I will introduce an example in fluid dynamics, falling liquid films, that, by being comparatively simple to the full problem modelled by the Navier–Stokes equations, allows us to construct feedback controls that stabilise the full system with a lower computational cost and with no need for the use of ROMs.

In what follows, I will first introduce the basic concepts and results on feedback control needed to do this, followed by a short section describing the physical problem and the various models I consider. I will conclude with a survey of recent results on the control of falling liquid films, thus illustrating how sometimes one can obtain several useful (albeit numerical) results that can have an influence on practical applications, even when we cannot prove analytical results because we do not have the necessary assumptions on the problem (such as global well-posedness), and finish with some open problems.

## 1 A SHORT INTRODUCTION TO CONTROL THEORY

In this section, I summarise the main results in (feedback) control theory which I will use later on. I will

\* **Mathematics Institute, University of Warwick. Email: [Susana.gomes@warwick.ac.uk](mailto:Susana.gomes@warwick.ac.uk)**

start with an ODE example and illustrate how these results translate to PDEs.

Consider, for simplicity, the example a scalar ODE

$$\dot{y} = \lambda y, \quad y(0) = y_0, \quad (1)$$

where the dot represents derivatives with respect to time. One can easily show that the solution of (1) is the function  $y(t) = y_0 e^{\lambda t}$ , and in particular, that  $y(t) \rightarrow 0$  if  $\lambda < 0$  and  $y(t) \rightarrow \infty$  if  $\lambda$  is positive.

An intuitive thing to do to *stabilise* the system (i.e., to drive it towards the solution  $y(t) = 0$ ), is to introduce a control (or forcing) term to equation (1), i.e., rewrite the controlled equation as

$$\dot{y} = \lambda y + f, \quad y(0) = y_0. \quad (2)$$

We can then choose  $f$  in such a way that the solution is *stabilised*, and it is easy to see that it suffices to use a simple *proportional feedback control*:  $f(t) = -\alpha y(t)$  for some positive constant  $\alpha$  so that  $\lambda - \alpha < 0$ . In this case, we say that the control  $f(t)$  stabilises the solution to the ODE. The term feedback is used because the control uses information on the current state of the system; the control is called *proportional* since it is proportional to the current solution.

Building up on this idea, we can consider the problem of controlling a *system* of ODEs, i.e., a problem of the form

$$\dot{\mathbf{y}} = A\mathbf{y} + \mathbf{f}, \quad \mathbf{y}(0) = \mathbf{y}_0, \quad (3)$$

where now  $\mathbf{y}, \mathbf{y}_0, \mathbf{f} \in \mathbb{R}^d$  and  $A$  is a  $d \times d$  matrix. It can be shown that in this case, when  $\mathbf{f} = \mathbf{0}$ , if all the *eigenvalues* of  $A$  have negative real part, the solution is *asymptotically stable*, i.e.,  $\mathbf{y}(t) \rightarrow \mathbf{0}$  as  $t \rightarrow \infty$ . The analogue of the previous control here is to use  $\mathbf{f}(t) = -\alpha \mathbf{y}(t) = -\alpha I \mathbf{y}(t)$ , where  $I$  is the  $d \times d$  identity matrix. A simple calculation can be used to find the smallest  $\alpha$  necessary to stabilise the system, namely, choose  $\alpha$  such that the eigenvalues of  $A - \alpha I$  all have negative real part.

While this is an easy thing to do, often in applications we can use information about the problem to obtain more efficient controls. Alternatively, it can be necessary to apply controls only to certain variables. This can be achieved by modifying the problem statement as follows:

$$\dot{\mathbf{y}} = A\mathbf{y} + B\mathbf{f}, \quad \mathbf{y}(0) = \mathbf{y}_0. \quad (4)$$

Here,  $B$  is a  $d \times M$  matrix that encodes some information about how one applies the controls—for example, one can have  $M$  *control actuators* (where each column of  $B$  represents the effect of one control), or have different controls affect some rows of the system and not others. In this case, the controls are  $\mathbf{f} \in \mathbb{R}^M$

(i.e. there are  $M$  of them). Note that we can have  $M = d$  and  $B = I$ , which is the case outlined above. It can be shown that under some assumptions on the matrices  $A$  and  $B$  (namely, the Kalman rank condition [23]), one can find a matrix  $K$  such that the eigenvalues of  $A + BK$  all have negative real part, and therefore the controls  $\mathbf{f} = K\mathbf{y}$  stabilise the system. The matrix  $K$  can be computed using a pole placement algorithm [12] or by solving a linear-quadratic regulator problem [23].

In several complex systems relevant to applications, the interest is to control nonlinear dynamics, and we instead have a nonlinear system of ODEs,

$$\dot{\mathbf{y}} = \mathcal{N}(\mathbf{y}) + B\mathbf{f}, \quad \mathbf{y}(0) = \mathbf{y}_0, \quad (5)$$

where  $\mathcal{N}$  is some nonlinear function of  $\mathbf{y}$ . Similar controllability or stabilisability results can be obtained (under assumptions on  $\mathcal{N}$  such as Lipschitz continuity) by considering a linearisation of the nonlinear operator and using Lyapunov function type arguments [23].

Finally, for several applications there is interest in controlling (linear or nonlinear) *partial differential equations* (PDEs); for example a reaction-diffusion equation for the evolution of a population, tumour growth or other biological and chemical applications. Such PDEs take the general form

$$u_t = \mathcal{L}u + \mathcal{N}(u) + f, \quad (6)$$

along with appropriate initial and boundary conditions. The subscript  $t$  denotes time derivative, and  $\mathcal{L}, \mathcal{N}$  are linear and nonlinear spatial differential operators, respectively. By projecting this equation to an appropriate basis (e.g., taking Fourier transforms), one can write the PDE as an *infinite-dimensional* system of ODEs such as (5). Alternatively, one can also discretise the problem (e.g. using finite differences) to rewrite it as a finite dimensional system of equations. This approach is commonly known as “discretise then optimise”. Passing to the PDE limit is not straightforward, even for linear PDEs [23]. However, in certain cases, this is possible; this is done for several linear PDEs (see [21]), and I will show a particular case of a nonlinear PDE in the next section.

## 2 FALLING LIQUID FILMS AND HOW TO CONTROL THEM

I will now introduce the problem of a falling liquid film, which is a canonical setting in fluid dynamics

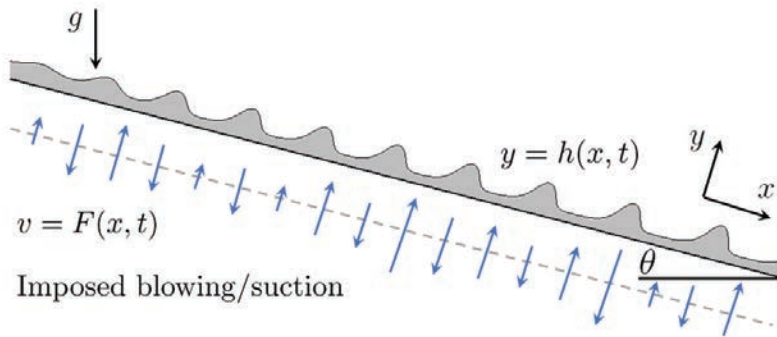


**Figure 1.**—Diagram of a thin film flowing down an inclined plane and allowing for blowing and suction controls. The dynamics of the interface  $y=h(x,t)$  are controlled by some fluid parameters, as well as the inclination angle  $\theta$  and the imposed control values  $v=F(x,t)$  at  $y=0$  in the coordinate system shown in the figure.

with applications such as coating of LCD screens or manufacturing of microchips.

## 2.1 A HIERARCHY OF MODELS FOR FALLING LIQUID FILMS

Falling liquid films are thin films of a viscous fluid flowing down an inclined plane, as shown in Figure 1. This problem has been studied extensively both theoretically (accurate model development, see, for example, [3, 11, 15]) and experimentally ([6]) and provides a set of models which is amenable to control development. The goal here is to control the interface towards a desired shape; for example, while the uncontrolled system evolves towards a travelling wave such as the one depicted in Figure 1, or more complex, and even chaotic, solutions, in applications such as LCD screen coating one would want the interface to be flat, whereas for microchip cooling we would desire a wavy interface with a suitable profile, to enhance heat transfer. For the models I will show, the flat solution will correspond to  $h(x, t) = 1$  unless otherwise stated. To control the resulting interface, we will allow for fluid to be inserted or removed from the system via slots at the plate that the film is flowing over, as depicted in Figure 1, and this will appear as a boundary condition, or as a coefficient in the different models we will consider. We will see how to design the controls, i.e., how to prescribe how much fluid is inserted or removed from the system at each slot, as well as how many of these controls we need,

using variations of the feedback control theory outlined in the previous section.

This physical problem is modelled by the (two-dimensional) Navier–Stokes equations;<sup>[1]</sup> in particular by modelling the interaction between the fluid and the air via the interface at  $y = h(x, t)$ . After an appropriate non-dimensionalisation, the system parameters are reduced to two non-dimensional groupings: the Reynolds number  $Re$  measuring the relative importance between inertia and viscosity, and the capillary number  $Ca$  which measures the importance of surface tension. The Navier–Stokes equations consist of the momentum equations for  $u$ ,  $v$ , and  $p$  the streamwise (parallel to the plane) and transverse (perpendicular to the plane) velocities, and pressure, respectively.

$$Re(u_t + uu_x + vv_y) = -p_x + 2 + u_{xx} + u_{yy}, \quad (7)$$

$$Re(v_t + uv_x + vv_y) = -p_y - 2 \cot \theta + v_{xx} + v_{yy}, \quad (8)$$

which are coupled to the continuity equation given by

$$u_x + v_y = 0. \quad (9)$$

In addition, the system is completed by its boundary conditions. We consider periodic boundaries in the  $x$ -direction<sup>[2]</sup>, no-slip and fluid injection/removal at the wall,

$$u = 0, \quad v = F(x, t), \quad (10)$$

the nonlinear dynamic stress balance (or momentum

<sup>[1]</sup> It is possible to generalise the problem to three dimensions, but this is much more computationally expensive, and for the purposes of this problem, a 2D description is often enough.

<sup>[2]</sup> This is a modelling assumption, which simplifies the analytical computations that follow. If the domain is sufficiently long, this is a good enough approximation, but different approaches can consider different boundary conditions.

jump) at the interface,  $y = h(x, t)$ ,

$$(v_x + u_y)(1 - h_x^2) + 2h_x(v_y - u_x) = 0, \quad (\text{I1})$$

$$p - \frac{2(v_y + u_x h_x^2 - h_x(v_x + u_y))}{1 + h_x^2} = \frac{1}{Ca} \frac{h_{xxx}}{(1 + h_x^2)^{3/2}}, \quad (\text{I2})$$

and finally the kinematic boundary condition

$$h_t = v - u h_x. \quad (\text{I3})$$

The uncontrolled system admits a uniform flat film solution known as the Nusselt solution [11], given by  $h(x, t) = 1$  and a semi-parabolic in  $y$  horizontal fluid velocity, which can be used to obtain simplified models.

It is well-known that full models such as the Navier–Stokes equations are computationally expensive to simulate, and therefore if one wants to solve it for several values of the relevant parameters (or, for example, perform optimal control using these models), it becomes prohibitively expensive. However, in the case of thin liquid films, the mean interface height is much smaller than the length of the domain,  $L$ , and this makes it possible to define a *long wave* parameter  $\epsilon = 1/L \ll 1$ . This disparity of scales facilitates a multiscale approach to derive from first principles hierarchies of simplified models. [3] To be able to derive these models, we need the following assumptions:

- (A1) (long-wave assumption) the geometrical aspect ratio  $\epsilon$  is small;
- (A2) The Reynolds number  $Re$  is  $\mathcal{O}(1)$ ;
- (A3) Surface tension is sufficiently strong to appear at leading order, i.e., the capillary number is small, and  $Ca = \mathcal{O}(\epsilon^2)$  is the appropriate distinguished limit;
- (A4) The controls  $F$  are small  $F = \mathcal{O}(\epsilon)$ , implying weak injection or removal of fluid via the control actuators.

Using assumptions (A1)–(A4) and asymptotic analysis techniques, Thompson *et al.* [20] derived two different long-wave models for falling liquid films using this type of control (long-wave models for uncontrolled falling liquid films were explored earlier in the literature, see [11]). Both models satisfy a mass conservation equation

$$h_t + q_x = F(x, t), \quad (\text{I4})$$

which is coupled with an equation for the flux  $q(x, t) = \int_0^h u(x, y, t) dy$ . In the first model, the *Benney equation*, they obtain an explicit expression for  $q(x, t)$  and the model is a single PDE for the interfacial height  $h(x, t)$ :

$$q(x, t) = \frac{h^3}{3} \left( 2 - 2h_x \cot \theta + \frac{h_{xxx}}{Ca} \right) + Re \left( \frac{8h^6 h_x}{15} - \frac{2h^4 F}{3} \right). \quad (\text{I5})$$

The second model is the *weighted residuals model*, which describes the evolution of the interfacial height  $h(x, t)$  and the flux  $q(x, t)$ :

$$\frac{2Re}{5} h^2 q_t + q = \frac{h^3}{3} \left( 2 - 2h_x \cot \theta + \frac{h_{xxx}}{Ca} \right) + Re \left( \frac{18q^2 h_x}{35} - \frac{34hqq_x}{35} + \frac{hqF}{5} \right). \quad (\text{I6})$$

We note that the controls appear as an inhomogeneous term  $F(x, t)$  in the mass conservation equation (I4), and this structure plays a crucial role in the efficiency of these controls.

Due to the asymptotic reduction, these models only provide us with the interface height  $h(x, t)$  and downstream flux  $q(x, t)$  and do not directly provide the solution to the Navier–Stokes equations (i.e.  $u$ ,  $v$ , and  $p$ ). However, if needed, these can be recovered from  $h$  and  $q$ , thus allowing for comparison with direct numerical simulations of the Navier–Stokes equations when necessary.

The above long-wave models are significantly more accessible computationally than the full Navier–Stokes equations, but they are still highly nonlinear. This means that it is hard (if not impossible) to treat them analytically, and to the best of my knowledge there are no analytical results beyond linear stability analysis of the flat solution (and some results on solitary waves for some special cases) [11]. Because of this, there is some interest in applying further simplifications in order to make analytical progress. For very small but nonlinear perturbations of the flat solution, one can perform weakly nonlinear analysis to derive a Kuramoto–Sivashinsky (KS) equation [11, 19]. The KS equation is a fourth-order nonlinear PDE having the same form as (6), and is given by

$$\eta_t + \nu \eta_{xxxx} + \eta_{xx} + \eta \eta_x = f(x, t),$$

where  $\eta$  is a small perturbation of a flat interface and  $\nu > 0$  is a parameter that encodes some of the

[3] We often call these reduced-order models, but I will not use this terminology, to avoid confusion with ROMs obtained via, e.g., PCA.

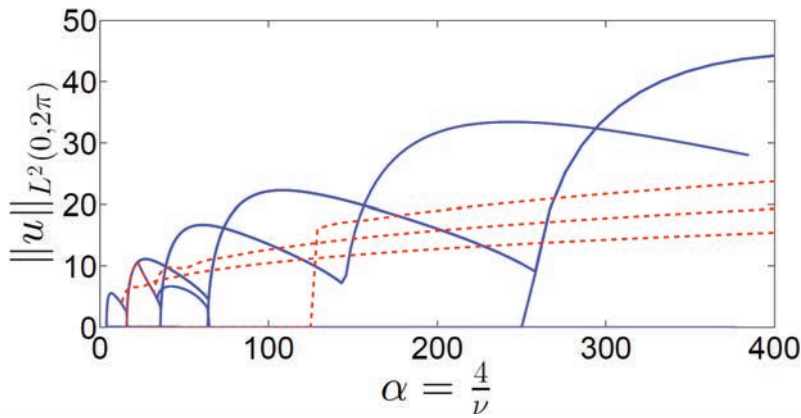


**Figure 2.**—Bifurcation diagram of the solutions of the KS equation. Full blue lines correspond to steady state solutions while dashed red lines are travelling waves. Not all branches are included, and most solutions depicted here are unstable.

geometry of the problem<sup>[4]</sup>. This problem is posed with periodic boundary conditions and we have  $x \in [0, 2\pi]$ . In this case, a flat interface corresponds to  $\eta = 0$ .

The KS equation appears in several applications and is widely studied since it is one of the simplest model PDEs exhibiting spatiotemporal chaotic behaviour. Over the last few decades, existence and uniqueness of solutions have been explored [17], different types of attractors have been characterised [5], and the route to chaos for solutions of the KS equation have been reported [13], to show a small subset of the range of interesting analytical and computational results that can be achieved even at this lowest member of the model hierarchy. It is possible to compare the results from these models to direct numerical simulations of the Navier–Stokes equations, and some relevant comparisons can be seen in [6]. While the long-wave models provide a very good approximation of the full system, in most cases the KS equation solution differs significantly from it (see Figure 2 in [4]). However, its simplicity and existing analytical results have allowed us to develop efficient controls (see [2, 8]) which were then extended to controlling long-wave models [19] and eventually the full model [4, 10]. For the rest of this article, I will summarise our results in this direction.

## 2.2 FEEDBACK CONTROL OF FALLING LIQUID FILMS

I will start outlining our results towards control of falling liquid films by showing the (analytical and numerical) results on controlling the KS equation. As mentioned above, while there is significant model error when considering this PDE to model interfaces of falling liquid films, the analytical insights can provide us with enough information to motivate control development on the more complicated long wave models, and eventually design controls that drive the solution to the full system towards a desired state.

The controlled KS equation, rewritten so that controls reflect a finite number of control actuators that inject and remove fluid through slots is given by

$$\eta_t + \nu \eta_{xxxx} + \eta_{xx} + \eta \eta_x = \sum_{j=1}^M \delta(x - x_j) f_j(t). \quad (17)$$

For the uncontrolled problem, it is easy to check that if  $\nu < 1$ , the zero solution is linearly unstable. Without the nonlinear term  $\eta \eta_x$ , the solution would grow exponentially in time; however, the nonlinearity promotes exchange of energy between Fourier modes and instead we see a “zoo” of solutions, from steady states, to travelling waves, but more generally we observe chaotic behaviour. This can be seen in Figure 2, where we plot the bifurcation diagram of possible solutions of the KS equation, with steady states depicted in full blue lines, and travelling waves by red

<sup>[4]</sup> Most of the geometry of the problem, however, is encoded in the change of variables used to arrive at this equation; in particular, the solutions of this equation sit on a moving frame, and so even “steady-state” solutions correspond to travelling waves of the original problem.

dashed lines. The  $y$  axis plots the  $L^2$  norm of different solutions (here  $u$  should be replaced by  $\eta$ ). The figure is taken from [8].

Armaou and Christofides showed in [2] that the zero solution of the KS equation in small domains ( $v$  close to 1) can be controlled using  $M = 5$  control actuators. More recently, we were able to show that we can stabilise any unstable solution (any of the branches depicted in Figure 2) of the KS equation using as many control actuators as unstable modes in the system (see [8, 9]).

To show this, it is useful to consider a discretisation of the KS equation. Let any solution be written as

$$\eta_t = \eta_0(t) + \sum_{k=0}^{\infty} \eta_k^s(t) \sin(kx) + \eta_k^c(t) \cos(kx).$$

We can then write the KS equation as an infinite system of ODEs for the coefficients  $\eta_k^*$  (where  $*$  stands for  $c$  or  $s$ ). Defining  $\boldsymbol{\eta} = (\eta_0, \eta_1^s, \eta_1^c, \dots)$ , this system is written as:

$$\dot{\boldsymbol{\eta}} = \mathcal{A}\boldsymbol{\eta} + \mathcal{N}(\boldsymbol{\eta}) + \mathbf{B}F,$$

where  $\mathcal{A}$  is a diagonal matrix whose entries are  $-vk^4 + k^2$ ,  $\mathcal{N}$  is given by a convolution,  $\mathbf{B}$  includes the discretisation of the control actuators ( $B_{kj} = \int_0^{2\pi} \delta(x - x_j) \sin(kx) dx$ , equivalently for the coefficient corresponding to  $\cos(kx)$ ), and  $F$  encodes the control action.

**PROPOSITION 1.**— Let  $\bar{\eta}$  be a linearly unstable steady state or travelling wave solution of the KS equation (17) and let  $2\ell + 1$  be the number of unstable eigenvalues of the operator  $\mathcal{A}$ , i.e.,  $\ell + 1 \geq 1/\sqrt{v} > \ell$ . Additionally, let  $A_u$  be the  $M \times M$  submatrix consisting of coefficients corresponding to unstable modes, and define  $B_u$  similarly. If  $M = 2\ell + 1$ , then there exists a matrix  $K \in \mathbb{R}^{M \times M}$  such that all of the eigenvalues of the matrix  $A_u + B_u K$  have negative real part, and the state feedback controls  $F = K(\boldsymbol{\eta} - \bar{\boldsymbol{\eta}})$  stabilise  $\bar{\boldsymbol{\eta}}$ .

**PROOF.**— I will only sketch the proof of this result; for more details see [7]. First, consider the problem of controlling the system of  $M$  ODEs

$$\dot{\mathbf{y}} = A_u \mathbf{y} + B_u F.$$

If each control actuator has a different location (i.e.  $x_i \neq x_j$ ), then it is easy to show that the columns of  $B_u$  are linearly independent, and therefore it can be shown that the matrices  $A_u$  and  $B_u$  satisfy the Kalman rank condition and the system is controllable. Therefore, we can guarantee that there exists a matrix  $K$

such that  $A_u + B_u K$  has negative eigenvalues. We can then use an algorithm such as pole placement [12] to find  $K$  – in particular, we will choose  $K$  such that all eigenvalues of  $A_u + B_u K$  have real part smaller than  $-\inf |\eta_x|/2$ .

Now we define the perturbation  $v = \bar{\eta} - \eta$  and write a PDE for  $v$ :

$$v_t + v v_{xxxx} + v_{xx} + v v_x + (\bar{\eta} v)_x = \sum_{j=0}^M \delta(x - x_j) f_j(t).$$

Multiplying this equation by  $v$  and integrating by parts, we obtain, formally,

$$\begin{aligned} \frac{1}{2} \frac{d\|v\|^2}{dt} &= \int_0^{2\pi} v(\mathcal{A} + \mathbf{B}K)v dx + \\ &+ \int_0^{2\pi} v^2 v_x + v(\bar{\eta} v)_x dx. \end{aligned}$$

The integral of  $v^2 v_x$  vanishes due to periodic boundary conditions. Furthermore, we can show that the term  $\int v(\bar{\eta} v)_x dx$  is bounded by  $\inf |\eta_x| \|v\|^2/2$ , and therefore it can be shown from the choice of eigenvalues that the right-hand side is bounded by  $-\lambda \|v\|^2$  where  $\lambda$  is the largest eigenvalue of  $A_u + B_u K$ , showing that  $\|v\|^2$  is a Lyapunov function for this system, and therefore  $v = 0$  is a stable solution, meaning  $\eta = \bar{\eta}$  is stabilised using the controls  $F = \mathbf{B}Kv = \mathbf{B}K(\eta - \bar{\eta})$ .

It can also be shown (see [8]) that the controls are robust to uncertainty in the problem parameters, as well as to small changes in the number of controls used. For an example of a controlled solution see Figure 3.

Motivated by the similar linear stability properties between the KS equation and the Benney equation (the simplest long-wave model), we studied the control problem for two long-wave models: the Benney equation and the weighted residual model in Thompson *et al.* [19]. We started by showing that in the unrealistic scenario where one can observe the whole interface and *actuate everywhere*, the simplest proportional controls of the form

$$f(x, t) = -\alpha(h(x, t) - 1), \quad (18)$$

for some constant  $\alpha > 0$  to be determined, efficiently drive the system towards the flat solution  $h(x, t) = 1$  (or indeed any desired solution  $H(x, t)$ , by replacing 1 by  $H(x, t)$ ). The critical value

$$\alpha_c = \frac{16Ca(Re - \frac{5}{4} \cot \theta)}{75}$$

can be computed from linear stability analysis of the Benney equation or the weighted residuals model,

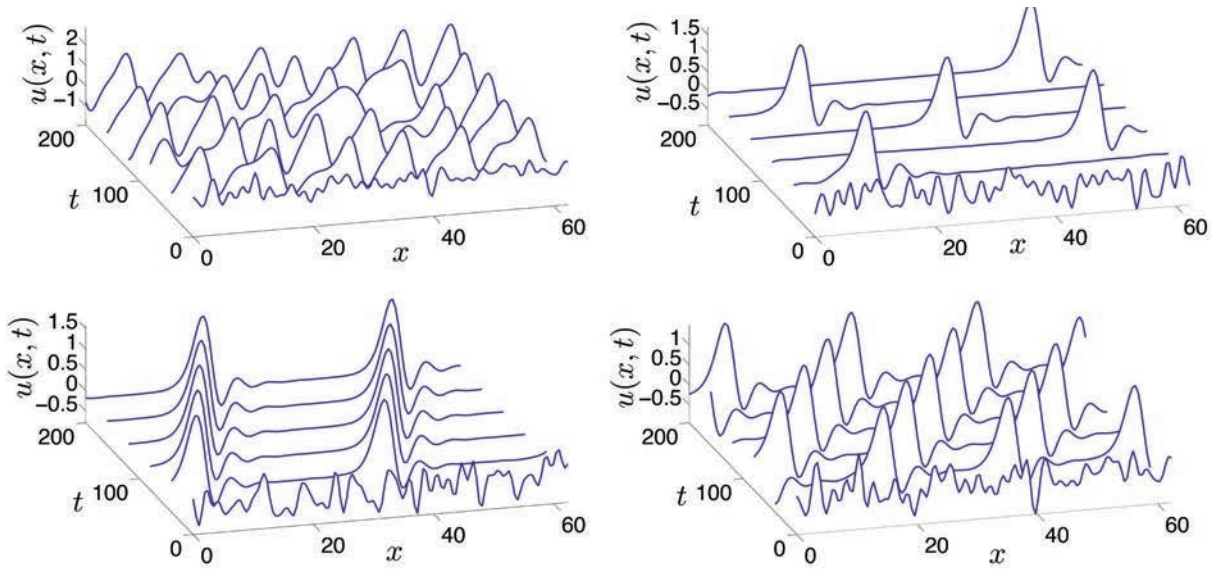


**Figure 3.**—Control of the KS equation for  $\nu=0.01$ . Uncontrolled solution showing chaotic behaviour (top left), and controlled solution towards: a 1-pulse travelling wave (top right), a 2-pulse travelling wave (bottom left), and a 3-pulse travelling wave (bottom right). We used  $M=21$  equidistant controls.

and it depends only on the Reynolds and capillary numbers. Using linear stability analysis, we can also calculate the number of unstable modes (see [10]) to be

$$M = 1 + 2\ell = 1 + 2 \left[ \frac{L}{2\pi} \sqrt{Ca \left( \frac{8}{5} Re - 2 \cot \theta \right)} \right]. \quad (19)$$

It is also shown in [19] that the critical  $\alpha$  for the Benney equation is sufficient to obtain linear stability of the weighted residuals model and indeed the full Navier–Stokes equations, by solving an Orr–Sommerfeld system. As mentioned before, in this case, because of the nonlinearities of the system, we cannot prove that linear stability of the controlled solutions guarantees that the solution of the long wave models or the Navier–Stokes equations will indeed be stabilised. However, we can confirm nonlinear stability of these solutions by numerical simulations of the initial value problem.

Similarly to the KS equation, one can compute point actuated controls assuming we can observe the whole interface (using pole placement or solving an LQR problem), and unsurprisingly controls of this type also stabilise the flat solution. A more interesting (and realistic) case is when we not only actuate at a finite number of locations, but can also only observe the interface at a finite number of points. In this case, in [19] we use proportional feedback controls of the form

$$f(x, t) = -\alpha \sum_{j=1}^M \delta(x - x_j) (h(x_j - \phi, t) - 1), \quad (20)$$

where  $\delta(\cdot)$  is the Dirac delta function, the control actuators are located at the positions  $x_j$ ,  $j = 1, \dots, M$ , and observations of the interface are made at  $x = x_j - \phi$  for some displacement  $\phi$ . Figure 4 shows predictions of whether these controls stabilise the nonlinear dynamics for  $L = 64$ ,  $\theta = \pi/3$ ,  $Re \approx 15$  and  $Ca \approx 0.001$  (3 unstable modes) using  $M = 3, 5, 7$ , or 9 and  $P = M$  observers with a displacement  $\phi$  from the corresponding actuator. We observe that positive  $\phi$ , i.e. observations upstream of actuation, are beneficial; this makes sense intuitively, since if we observe upstream, we can predict where the wave will be by the time the control effects reach it.

Again, linear stability does not guarantee the solution of the nonlinear equation will be stabilised, but for most cases, we can confirm numerically that this is the case. I will show examples of this when applied to the full model (the Navier–Stokes equations) in the next section.

### 2.3 APPLYING THE CONTROLS TO THE FULL MODEL

Now that we have efficient controls that stabilise the KS equation and the long wave models, we are ready to apply these to the full Navier–Stokes equations. As mentioned previously, the full system is quite complex, and hard to simulate. To test the controls, we perform direct numerical simulations (DNS) of the Navier–Stokes equations using the open-source software Gerris [14] and its extension Basilisk, which solve the Navier–Stokes equations on an adaptive quadtree grid using a volume-of-fluid approach.

The control strategies developed in the previous

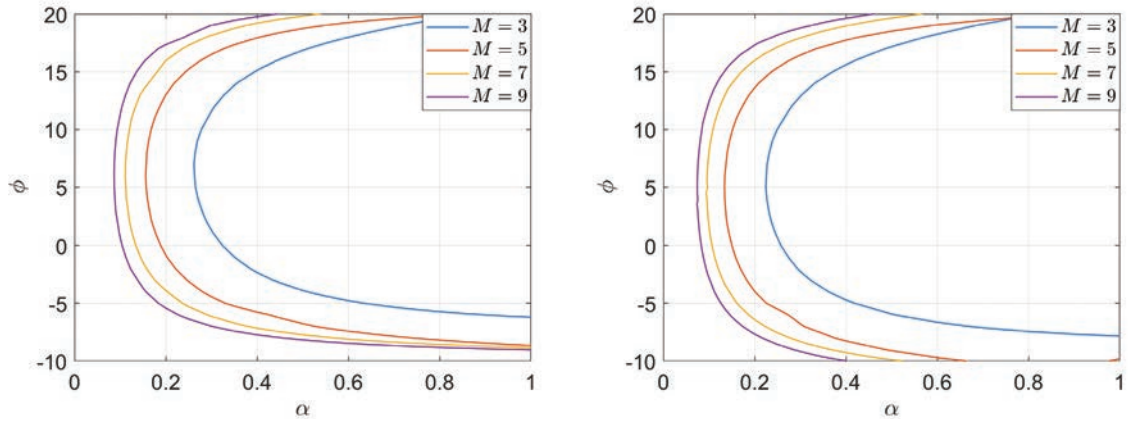


**Figure 4.**—Regions of stability of controls of the form (20) for several number of controls  $M$  and displacement  $\phi$ . Left: Benney equation, and right: weighted residuals model. Inside each curve, we predict the controls to stabilise the flat solution, while outside we predict them to not be sufficient for stability.

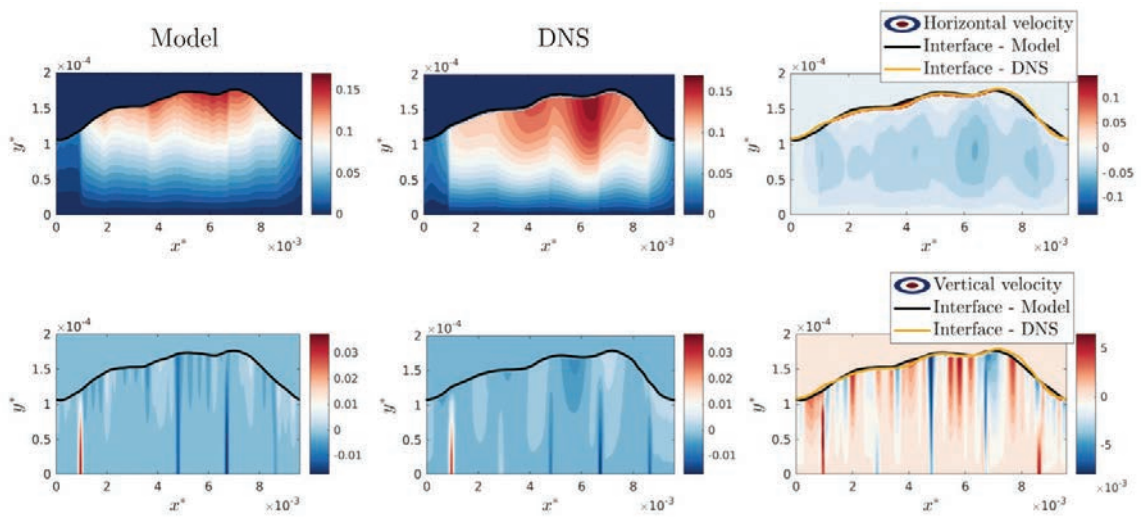


**Figure 5.**—Comparison between the solution,  $(u, v)$ , of the Navier–Stokes equations using approximations obtained from the weighted residuals model (left) and DNS (middle), and the difference between the two (right) for the horizontal velocity  $u$  (top) and the vertical velocity  $v$  (bottom), immediately after application of controls. For details on the parameters used, see [4].

section are efficient in stabilising the flat solution for the Benney equation and the weighted residuals model, and linear stability analysis predicts they also (linearly) stabilise the full problem. Naively, we could try to use them directly in the Navier-Stokes equations; however, we observe that we cannot simply “translate” the controls directly to the full problem, i.e., simply take the numerical value from the simplified models and apply it to the Navier-Stokes equations: while they seem to work on the first few time steps, after a while the differences between the full problem and the simplified models become too big, the controls stop working, and the solution eventu-

ally returns to the original uncontrolled state. This is to be expected, since there are physical effects that appear at the DNS level which are not fully resolved in the weighted residuals model because of the physical assumptions we made to derive the models.

To illustrate this, we show a comparison in Figure 5 between the solution,  $(u, v)$ , of the Navier-Stokes equations using approximations obtained from the model (left) and DNS (middle), as well as the difference between the two (right) for the horizontal velocity  $u$  (top) and the vertical velocity  $v$  (bottom), immediately after application

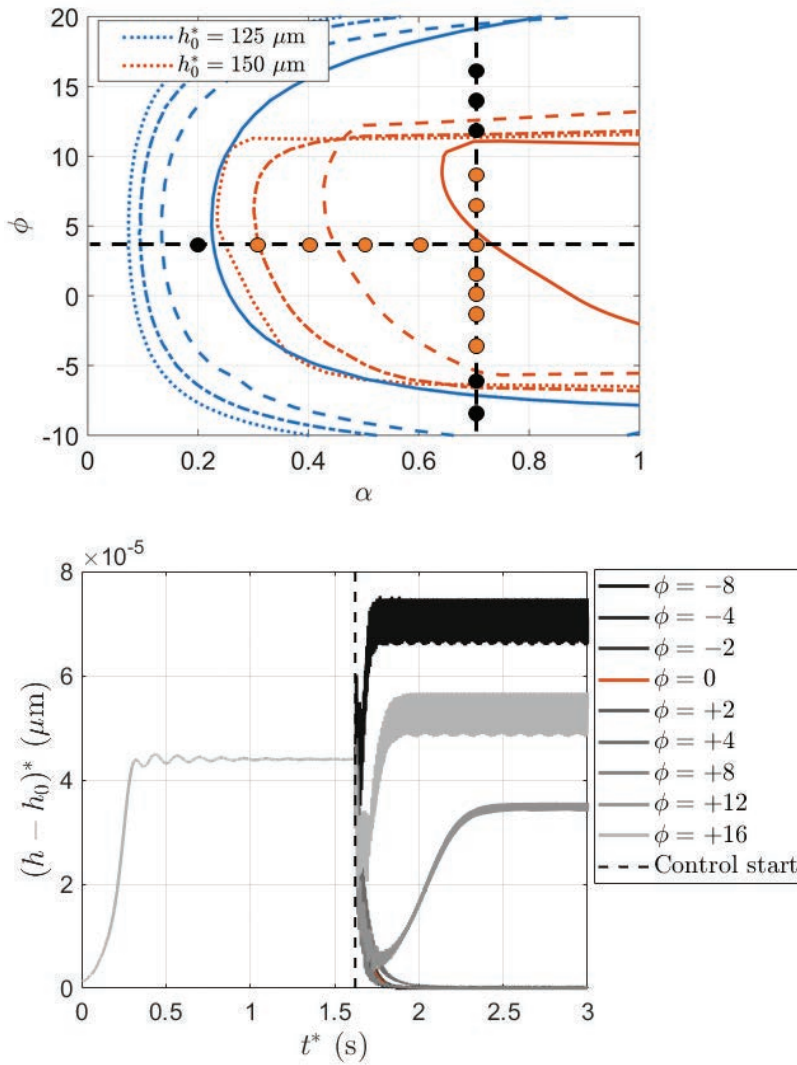


**Figure 6.**—Stability predictions (top) and direct numerical simulations (bottom) for the controlled solution of the Navier-Stokes equations for several values of  $\alpha$ .

of controls. We can see that even though the error on the horizontal velocity is small, there are significant differences in the vertical velocity.

However, we can use the linear stability analysis predictions (such as the control strategy in (20) with the predictions for  $\alpha$  visible in Figure 4) and apply these controls based on observations of the numerical solution obtained via the direct numerical simulations.

We tested this methodology for several cases, with  $L = 64$ ,  $\theta = \pi/3$  and including  $Re \approx 10$ ,  $Ca \approx 0.001$  (case 1), and  $Re \approx 17$ ,  $Ca \approx 0.001$  (case 2), with the results shown in Figure 6, where we show the stability predictions for case 1 in blue, and case 2 in orange (top figure). The different curves correspond to a different number of control actuators and observers varying from  $M = 3$  (full lines) to  $M = 9$  (dotted lines). In the bottom figure, we pick case 2 and  $M = 5$  con-

trols, and apply controls with varying  $\phi$  and fixed  $\alpha$ . Each curve corresponds to a dot on the vertical line in the top figure, where orange dots signify a stabilised solution, while black dots correspond to a failed control. We see that the direct numerical simulations confirm that controls predicted to linearly stabilise the weighted residuals model do indeed stabilise the full problem. We also performed similar tests for fixed  $\phi$  and varying  $\alpha$  with similar results.

Our final result concerns applying the controls derived for the long wave models to direct numerical simulations of the Navier-Stokes equations. As above, we use the control “rule” derived from linear stability analysis (in this case, solving an LQR Problem for the weighted residuals model), but where we use observations of the DNS solution. Motivated by the success of the controls in Figure 6, we expect the same philosophy to be applicable. We tested a range of Reynolds

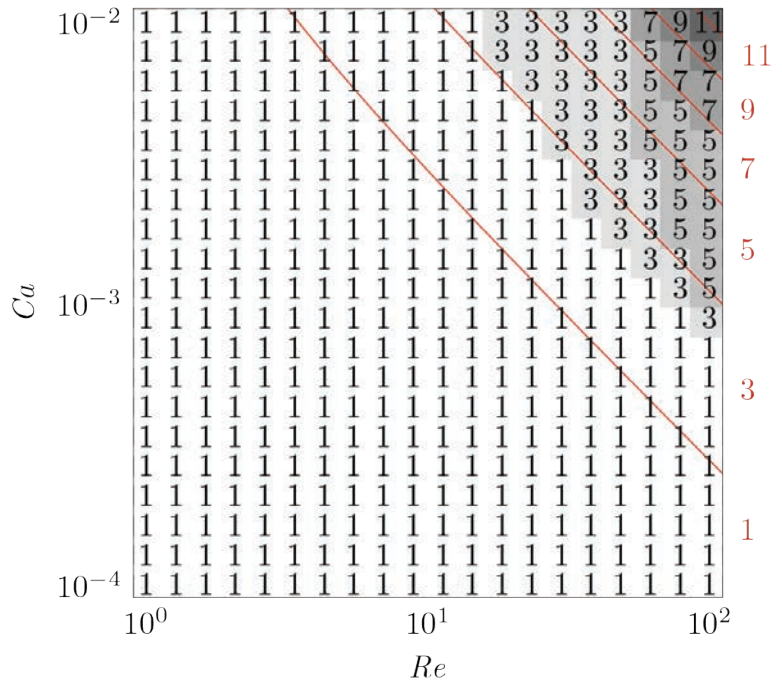


**Figure 7.**—The minimum number of actuators required to stabilise the Navier-Stokes film compared to the number of unstable modes of the linearised weighted-residual system (red). The number of controls needed to stabilise the uniform film never exceeds the number of unstable modes of the linear system  $M$  as given in (19). The ranges for the two parameters cover a broad range of different fluids. For more details, see [10].

numbers  $Re$  and capillary numbers  $Ca$  which correspond to several physically motivated fluids (see [10] for more details). For each case, we predicted the number of unstable modes — and therefore the number of necessary controls — using (19) and computed the matrix  $K$  from the weighted residuals model. We then applied the controls to the full model using observations from the DNS. The results are summarised in Figure 7: the red lines show the predicted number of controls, and the numbers in each square show how many controls were needed to stabilise the flat solution. We observe that in almost every case, we did not need as many controls as linear stability suggests, thus showing the efficiency of the controls we designed.

### 3 DISCUSSION

I presented a control methodology based on a hierarchy of models, which I used to control a canonical problem in fluid dynamics: falling liquid films. This is a complex problem for which control is hard due to the computational and analytical complexity of the models involved. Using a hierarchy of models allowed me to start from a weakly nonlinear model (the

Kuramoto-Sivashinsky equation), where it is possible to derive controls analytically that stabilise the flat solution, and any other unstable solution.

While the KS equation is not a very good approximation to the original problem, the results at this level provide crucial information to guide us in the right direction for controlling the more accurate long wave models (Benney equation and weighted residuals model), and eventually the Navier–Stokes equations.

The results I presented are based on linear feedback control theory, and can be thought of as a “discretise-then-optimize” framework. Other approaches can be used; for example, we can first optimize and then discretise, as seen, e.g., in [1], or we can use optimal control methodologies (see [22]). We can also use other forms of control such as electric fields [22] or temperature [18].

This illustrates how simple mathematical models are key players in mathematical studies and help us push conceptual boundaries to the point where the developed methodologies can be applied higher up in the model hierarchy. Often in control theory, several problems are not explored enough due to their non-linearity, which makes analytical progress impossible, and I hope this example shows the value of mathe-

mathematical modelling and numerical simulation working together with control theory to advance our understanding of complex phenomena in fluid dynamics.

## REFERENCES

- [1] R. Al Jamal and K. Morris. Linearized stability of partial differential equations with application to stabilization of the kuramoto–sivashinsky equation. *SIAM Journal on Control and Optimization*, 56(1):120–147, 2018.
- [2] A. Armaou and P. D. Christofides. Feedback control of the kuramoto–sivashinsky equation. *Phys. D*, 137(1-2):49–61, 2000.
- [3] D. J. Benney. Long waves on liquid films. *J. Math. Phys.*, 45(1-4):150–155, 1966.
- [4] R. Cimpanu, S. N. Gomes, and D. T. Papageorgiou. Active control of liquid film flows: beyond reduced-order models. *Nonlinear Dyn.*, 104(1):267–287, 2021.
- [5] P. Collet, J.-P. Eckmann, H. Epstein, and J. Stubbe. A global attracting set for the kuramoto–sivashinsky equation. 1993.
- [6] F. Denner, A. Charogiannis, M. Pradas, C. N. Markides, B. G. M. van Wachem, and S. Kalliadas. Solitary waves on falling liquid films in the inertia-dominated regime. *J. Fluid Mech.*, 837:491–519, 2018.
- [7] S. N. Gomes, S. Kalliadas, D. T. Papageorgiou, G. A. Pavliotis, and M. Pradas. Controlling roughening processes in the stochastic kuramoto–sivashinsky equation. *Phys. D*, 348:33–43, 2017.
- [8] S. N. Gomes, D. T. Papageorgiou, and G. A. Pavliotis. Stabilizing non-trivial solutions of the generalized kuramoto–sivashinsky equation using feedback and optimal control. *IMA J. Appl. Math.*, 82(1):158–194, 2017.
- [9] S. N. Gomes, M. Pradas, S. Kalliadas, D. T. Papageorgiou, and G. A. Pavliotis. Controlling spatiotemporal chaos in active dissipative-dispersive nonlinear systems. *Phys. Rev. E*, 92(2):022912, 2015.
- [10] O. A. Holroyd, R. Cimpanu, and S. N. Gomes. Linear quadratic regulation control for falling liquid films. *arXiv preprint arXiv:2301.11379*, 2023.
- [11] S. Kalliadas, C. Ruyer-Quil, B. Scheid, and M. G. Velarde. *Falling liquid films*, volume 176. Springer Science & Business Media, 2011.
- [12] J. Kautsky, N. K. Nichols, and P. Van Dooren. Robust pole assignment in linear state feedback. *International Journal of control*, 41(5):1129–1155, 1985.
- [13] D. T. Papageorgiou and Y. S. Smyrlis. The route to chaos for the kuramoto–sivashinsky equation. *Theoretical and Computational Fluid Dynamics*, 3(1):15–42, 1991.
- [14] S. Popinet. Gerris: a tree-based adaptive solver for the incompressible euler equations in complex geometries. *J. Comput. Phys.*, 190(2):572–600, 2003.
- [15] G. I. Sivashinsky and D. M. Michelson. On irregular wavy flow of a liquid film down a vertical plane. *Prog. Theor. Phys.*, 63(6):2112–2114, 1980.
- [16] E. D. Sontag. *Mathematical control theory: deterministic finite dimensional systems*, volume 6. Springer Science & Business Media, 2013.
- [17] E. Tadmor. The well-posedness of the kuramoto–sivashinsky equation. *SIAM Journal on Mathematical analysis*, 17(4):884–893, 1986.
- [18] A. B. Thompson, S. N. Gomes, F. Denner, M. C. Dallaston, and S. Kalliadas. Robust low-dimensional modelling of falling liquid films subject to variable wall heating. *Journal of Fluid Mechanics*, 877:844–881, 2019.
- [19] A. B. Thompson, S. N. Gomes, G. A. Pavliotis, and D. T. Papageorgiou. Stabilising falling liquid film flows using feedback control. *Phys. Fluids*, 28(1):012107, 2016.
- [20] A. B. Thompson, D. Tseluiko, and D. T. Papageorgiou. Falling liquid films with blowing and suction. *J. Fluid Mech.*, 787:292–330, 2016.
- [21] F. Tröltzsch. *Optimal control of partial differential equations: theory, methods, and applications*, volume 112. American Mathematical Soc., 2010.
- [22] Alexander W. Wray, Radu Cimpanu, and Susana N. Gomes. Electrostatic control of the navier-stokes equations for thin films. *Phys. Rev. Fluids*, 7:L122001, 2022.
- [23] J. Zabczyk. *Mathematical control theory: an introduction*. Birkhäuser, 1992.